

Effect of Temperature Gradient within Solid Particles for Dispersed Two-Phase Flow and Heat Transfer

*Takaaki TSUTSUMI¹, Shintaro TAKEUCHI², and Takeo KAJISHIMA²

¹Graduate School of Osaka University, Osaka University, Japan

²Department of Mechanical Engineering, Osaka University, 2-1 Yamada-oka, Suita-city, Osaka 565-0871, Japan

*Corresponding author: tsutsumi@fluid.mech.eng.osaka-u.ac.jp

Abstract

Liquid-solid two-phase flow with heat transfer is directly simulated to investigate the effect of temperature gradient within the solid objects. The interaction between fluid and particles is solved by our original immersed solid approach on a rectangular grid system. And a discrete element model with soft-sphere collision is applied for particle-particle interaction. A new heat conduction model is proposed for the heat conduction at the solid-liquid interface by considering the interface direction. The method is applied to liquid-solid two-phase flows in a confined square domain with a hot bottom plate and a cold top plane under a relatively low Rayleigh number. In dense condition, the particles of high heat conductivity induce strong convection and promote the heat transfer, while the particles of low heat conductivity depress the incoming heat flux from the bottom wall, resulting in low Nusselt number. The above simulation results highlight the importance of temperature distributions within the particles and liquid.

Keywords: Multiphase flow, Solid dispersion, Immersed solid object, Thermal flow, Heat conductivity

Introduction

Solid-dispersed two phase flows often involve heat (and mass) transfer through the interface. Temperature distributions in both fluid and solid phases play important roles on the fluid-solid interaction.

For numerical simulation of heat transfer problem in a flow including multiple solid objects, an immersed boundary method has an advantage. Kim et al. (2001) and Kim and Choi (2004) proposed a heat source/sink method for imposing iso-thermal and iso-heat-flux boundary conditions at the immersed boundary of a fixed particle. Similar approaches were proposed by Pacheco and co-workers (Pacheco, Pacheco-Vega, Rodić and Peck, 2005; Pacheco-Vega, Pacheco, Rodić, 2007) with a successive determination algorithm of the temperatures inside the body to match the iso-thermal and iso-heat-flux conditions at the immersed boundary. Ren et al. (2012) proposed an implicit formulation of the momentum and heat source/sink approach. The boundary force and heat flux are solved implicitly so that the no-slip and fixed temperature conditions are enforced on the immersed boundary.

The above researchers simplify the problem by imposing a boundary condition of either constant temperature or constant flux. And, there are few previous studies that deal with a conjugate heat transfer problem (convective and conductive heat transfers) in a two-phase flow including freely-moving particles (Yu, Shao and Wachs, 2006; Ueyama, Moriya, Nakamura and Kajishima, 2011).

In the present work, we study a heat transfer problem in a multiphase flow of dispersed solid particles including the effect of local heat flux at the liquid-solid surface (and therefore temperature gradient within the solid object). To facilitate the treatment of interaction problem between the fluid and a large number of relatively moving particles, a fixed grid approach is adopted.

The interaction between fluid and particles is solved with our original immersed solid approach (Kajishima, Takiguchi, Hamasaki and Miyake, 2001; Yuki, Takeuchi and Kajishima, 2007) on a rectangular grid system. The method employs a simple procedure for the momentum-exchange by imposing a volume force (as an interaction force) on both solid and fluid phases. The method has been applied for studying a clustering process with a total of 1000 spherical particles in a turbulent flow (Kajishima, Takiguchi, Hamasaki and Miyake, 2001; Kajishima and Takiguchi, 2002; Kajishima, 2004). Also the usefulness of our method has been demonstrated by Nishiura et al. (Nishiura Shimosaka, Shirakawa, and Hidaka, 2006) through the analysis of sedimentation process employing a total of 10^5 spherical particles. In the present study, to include the effect of conjugate heat transfer in a liquid-solid interaction problem, a heat flux decomposition model is proposed for the heat conduction at the liquid-solid interface. The model employs a procedure for solving the temperature field in an Eulerian frame by considering the interface direction.

The present method is applied to a direct numerical simulation of laminar natural convection of relatively low Rayleigh number in a confined square domain including multiple particles of round shape. By including the particles of different ratios of heat conductivity (solid to liquid), we look into the effect of the solid temperature distribution on the behaviour of the particles, and the heat transfer mechanism is studied in the solid-dispersed two-phase flow field.

Governing Equations and numerical Methods

Governing equations

The governing equations for fluid are the equations of continuity, momentum and energy:

$$\nabla \cdot \mathbf{u}_f = 0, \quad (1)$$

$$\rho_f \frac{\partial \mathbf{u}_f}{\partial t} + \rho_f \mathbf{u}_f \cdot \nabla \mathbf{u}_f = -\nabla p + \mu_f \nabla^2 \mathbf{u}_f + \rho_f \beta (T - T_0) \mathbf{g}, \quad (2)$$

$$\frac{\partial \rho_f c_f T_f}{\partial t} + \mathbf{u}_f \cdot \nabla (\rho_f c_f T_f) = \nabla \cdot (\lambda_f \nabla T_f). \quad (3)$$

Here, an incompressible fluid is assumed and Boussinesq approximation is employed to include the effect of density fluctuation. In the following, viscous coefficient (μ_f), heat capacity per unit volume ($\rho_f c_f$) and thermal conductivity (λ_f) are assumed to be constant.

Fluid-solid interaction model: Immersed solid approach

Momentum exchange at the fluid-solid interface is solved by an immersed solid approach developed by Kajishima and the co-workers (Kajishima, Takiguchi, Hamasaki and Miyake, 2001; Kajishima and Takiguchi, 2002; Kajishima, 2004), on a uniformly distributed fixed grid system. This is briefly described below.

A velocity field \mathbf{u} is established through volume-averaging the local fluid velocity \mathbf{u}_f and the local particle velocity \mathbf{u}_p in a cell:

$$\mathbf{u} = (1 - \alpha) \mathbf{u}_f + \alpha \mathbf{u}_p, \quad (4)$$

where α ($0 \leq \alpha \leq 1$) is the local solid volume fraction in the cell. The particle velocity \mathbf{u}_p is decomposed into translating and rotating components as $\mathbf{u}_p = \mathbf{v}_p + \boldsymbol{\omega}_p \times \mathbf{r}$. This mixture velocity field \mathbf{u} is assumed to obey the following equation:

$$\frac{\partial \mathbf{u}}{\partial t} = -\frac{\nabla p}{\rho_f} + \mathbf{H}_u + \beta (T - T_0) \mathbf{g} + \mathbf{f}_p. \quad (5)$$

Interaction term \mathbf{f}_p works to assign the mixture velocity that satisfies the non-slip boundary condition at the interface (Kajishima, Takiguchi, Hamasaki and Miyake, 2001; Kajishima and Takiguchi, 2002; Kajishima, 2004). For time-update, the 2nd-order Adams-Bashforth and Crank-Nicolson methods are employed for the convective and viscous terms, respectively. The pressure gradient term in Eq. (5) is treated implicitly by a fractional step method. With the corrected velocity field $\tilde{\mathbf{u}}$, the fluid-solid interaction term \mathbf{f}_p is modelled as:

$$\mathbf{f}_p = \alpha \frac{(u_p - \tilde{u})}{\Delta t}, \quad (6)$$

where Δt is the time increment.

For motion of the particles, Newton's equations for momentum and angular momentum are solved. The same force as Eq. (6) applies to the fraction of the solid in the cell with the opposite sign. The surface integration of the hydrodynamic forces is changed to the integration of \mathbf{f}_p over the volume of the particle V_p :

$$m_p \frac{v_p^{n+1} - v_p^n}{\Delta t} = \int_{V_p} (-\rho_f \mathbf{f}_p) dV + \mathbf{G}_p, \quad (7)$$

$$\mathbf{I}_p \frac{\omega_p^{n+1} - \omega_p^n}{\Delta t} = \int_{V_p} \mathbf{r} \times (-\rho_f \mathbf{f}_p) dV + \mathbf{N}_p. \quad (8)$$

The above replacement from surface to volume integrations considerably facilitates the computation of the solid motion, and also the use of the same body force \mathbf{f}_p for both (fluid and particle) phases in a shared Cartesian cell ensures no leakage of momentum between the phases. Eqs. (7) and (8) are solved with a predictor-corrector method (Ueyama, Moriya, Nakamura and Kajishima, 2011).

Temperature field and interfacial heat conduction

Temperature field is treated in an Eulerian way irrespective of the substance occupying the cell. The numerical simulation are conducted under $\rho_s = \rho_f (= \rho)$ and $c_s = c_f (= c)$. The following equation is solved with heat flux \mathbf{q} :

$$\frac{\partial \rho c T}{\partial t} + \mathbf{u} \cdot \nabla (\rho c T) = -\nabla \cdot \mathbf{q}. \quad (9)$$

In the present work, \mathbf{q} is given by a single equation that covers both phases as well as the interface. The discretised temperature gradient $\nabla T|_{ij}$ at (i, j) cell is decomposed into surface-normal component $(\mathbf{nn}) \cdot \nabla T|_{ij}$ and tangential component $(\mathbf{I} - \mathbf{nn}) \cdot \nabla T|_{ij}$. In an interfacial cell partially occupied by the solid object (local solid volume fraction α), the following mean heat conductivities are defined in the surface normal and tangential directions, respectively:

$$\frac{1}{\lambda_n} = \frac{1-\alpha}{\lambda_f} + \frac{\alpha}{\lambda_p}, \quad (10)$$

$$\lambda_a = (1 - \alpha)\lambda_f + \alpha\lambda_p. \quad (11)$$

Assuming that the solid and fluid temperatures match with each other at the interface, the heat flux (covering the interfacial cell) \mathbf{q} is given by the following formula:

$$\mathbf{q} = -\lambda_n (\mathbf{nn}) \cdot \nabla T|_{ij} - \lambda_a (\mathbf{I} - \mathbf{nn}) \cdot \nabla T|_{ij}. \quad (12)$$

Eq. (9) is time-updated with the Crank-Nicolson method for diffusion term with the treatment of Eq. (12). This semi-implicit scheme stabilises the computation and enables simulation with particles of very high/low heat conductivities.

Interparticle and particle-wall collision model

A soft-sphere model is used to allow multiple-body collisions for interparticle and particle-wall collisions. A spring and dashpot model is employed to calculate the contact forces. In the present study, the same parameter values as Tsuji et al. (1993) are used for the spring constant, restitution coefficient and friction coefficient.

Tsuji et al. (1993) suggested the following condition for determining the time increment to sufficiently resolve the eigen oscillation of the mass-spring system:

$$\Delta t \leq \frac{\pi}{n} \sqrt{\frac{m_p}{k}} \quad (n \geq 10) . \quad (13)$$

In the present study, the smallest value of the right hand side of the above equation is found to be 1.47×10^{-3} for the smallest m_p employed in the following section. Considering the numerical accuracy of the momentum and energy equations from our preliminary study, the time increment is fixed to $\Delta t = 5.0 \times 10^{-4}$, hereafter.

In the present study, no heat exchange or heat source is modelled in the interparticle collisions.

Results and discussion

Solid-dispersed two-phase flow under natural convection is studied for different heat conductivity ratios (solid to fluid). The non-dimensional numbers used are Rayleigh number (Ra) and Prandtl number (Pr).

In the present work, the computational domain is a square shape of side length L , and the particles are initially arranged regularly in the domain. Temperature difference between the top and bottom wall is kept constant ($\Delta T = 1$), and no heat flux is given at the lateral walls. The non-slip condition and the Neumann condition are applied for the velocity and pressure, respectively, on the solid walls. The equations are non-dimensionalised with the reference length L , the reference velocity $U = \sqrt{g\beta\Delta TL}$, the reference pressure $\rho_f U^2$ and the characteristic temperature difference ΔT . To investigate the natural convection on the particles behaviour and heat transfer, Prandtl number, density ratio, and specific heat ratio are set to unity.

In the following, interaction between the fluid and particles is simulated with different ratios of heat conductivity.

Dense case with bulk solid volume fraction 38.5% (2-D)

Table1: Simulation parameters.

Number of grids	$N_x \times N_y$	200×200
Spatial resolution	D_p/Δ	10
Number of particles	N_p	14^2
Diameter of particles	D_p	$0.05L$
Rayleigh number	Ra	1.0×10^5
Heat conductivity ratio	λ_s/λ_f	$10^{-3}, 10^0, 10^1, 10^2, 10^3$

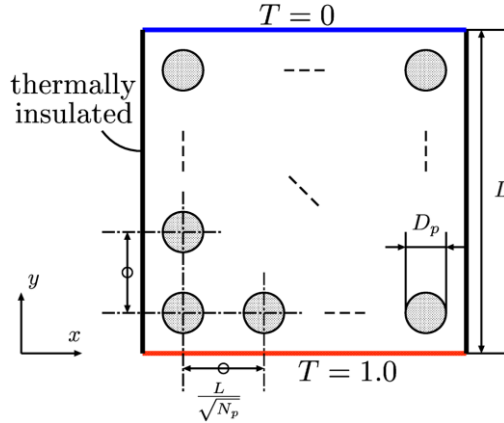


Figure 1: Schematic of arrangement of particles.

We look into the effect of the heat conductivity ratio on the particle motion in a natural convection of Rayleigh number 10^5 . The particles are initially arranged regularly in the domain as illustrated in Figure 1. The other parameters are summarised in Table 1. The bulk solid volume fraction is 38.5%. Figure 2 shows instantaneous flow and temperature fields at $t = 1000$ by employing the particles of $\lambda_s/\lambda_f = 10^{-3}$ and 10^3 . In both cases, the particles and fluid are found to constantly circulate in one direction around the domain centre after the initial developing stage. However, the local concentrations of the particles and time-averaged flow fields are different for the two cases. Figure 3 and 4 compare the time-averaged temperature and velocity fields and the time-averaged local solid volume fraction in each cell, respectively, for the two heat conductivity ratios.

For the particles of $\lambda_s/\lambda_f = 10^{-3}$, as shown in Figure 2(a), temperature gradient within the particle hardly re-distributes within the particle or to the fluid. From Figures 3(a) and 4(a), the concentrated isothermal lines and a region of high number density of the particles is found near the top and bottom walls. These suggest that, once a layer of particles is formed in those regions, the particles of poor-conductivity intercept the heat exchange with the walls. Therefore, low heat conduction in the particle could cause weak fluid convection and low Nusselt number.

On the other hand, for the case of $\lambda_s/\lambda_f = 10^3$, the particles efficiently transfer the heat to ambient fluid and generate temperature gradient in the fluid phase, resulting in strong fluid convection as observed in Figure 3(b). It is also characteristic, from Figure 4(b), that a region of low number density of the particles is found near the domain centre due to high rotating speed of the particulate flow and number density of the particles is distributed evenly except for the domain centre.

The heat transfer rate in two-phase natural convection system is compared for different particle conductivities. For evaluating heat transfer rate, the following Nusselt number is used with the heat flux at the hot (bottom) wall:

$$\text{Nu} = \frac{1}{\Delta T} \int_0^L \left(-\frac{\partial T}{\partial y} \right)_{y=0} dx . \quad (14)$$

Figure 5 compares the time evolutions of Nusselt number for five different λ_s/λ_f cases. The average level of the Nusselt number is found to increase as the heat conductivity ratio increases.

The above results show that the solid heat conductivity largely influences the flow pattern in solid dispersed two-phase flows and that the circulation of the particles enhances the heat transfer rate by transporting the heat from bottom to top.

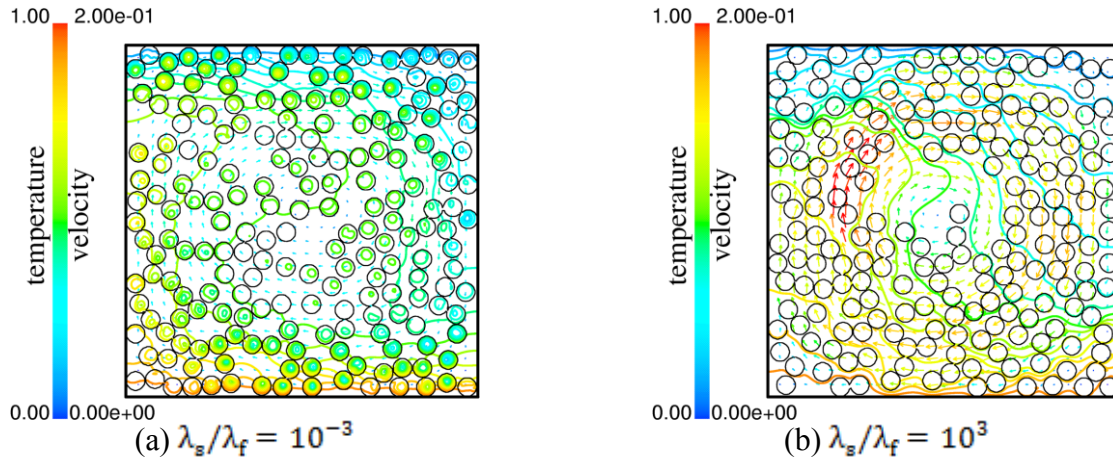


Figure 2: Instantaneous flow field and contours of temperature for different heat conductivities. Rayleigh number is 10^5 and bulk solid volume fraction is 38.5%. Colour shows the magnitude of the fluid velocity and iso-contour of temperature.

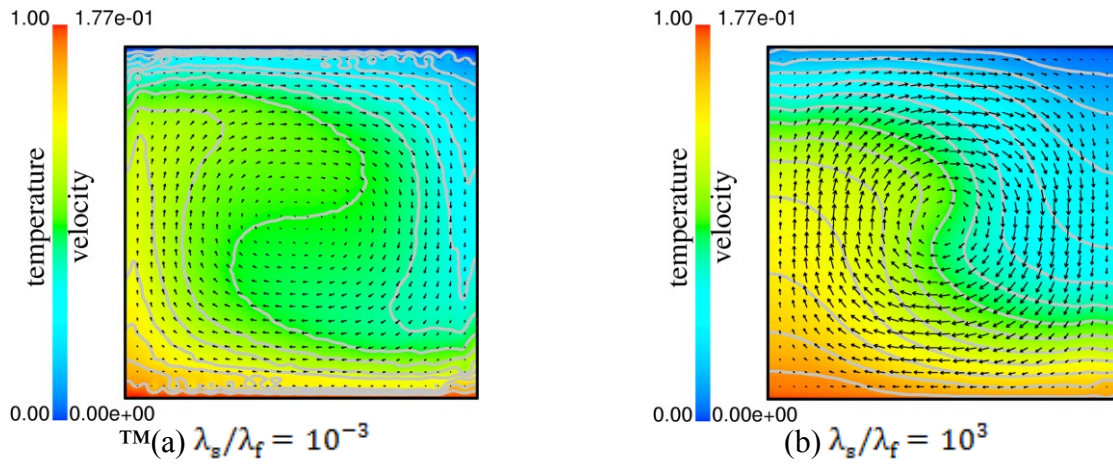


Figure 3: Time-averaged temperature and velocity fields for different heat conductivities. Rayleigh number is 10^5 . Average is taken between $t = 500$ and 1500 . Magnitude the fluid velocity are levelled by colour, and iso-contours of temperature are plotted at constant intervals.

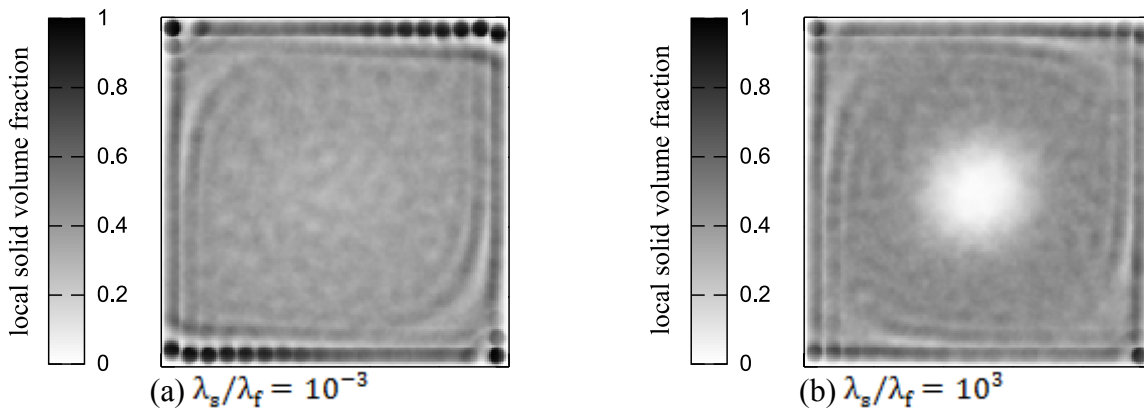


Figure 4: Time-average local solid volume fraction in a cell for different heat conductivities. Average is taken between $t = 500$ and 1500 .

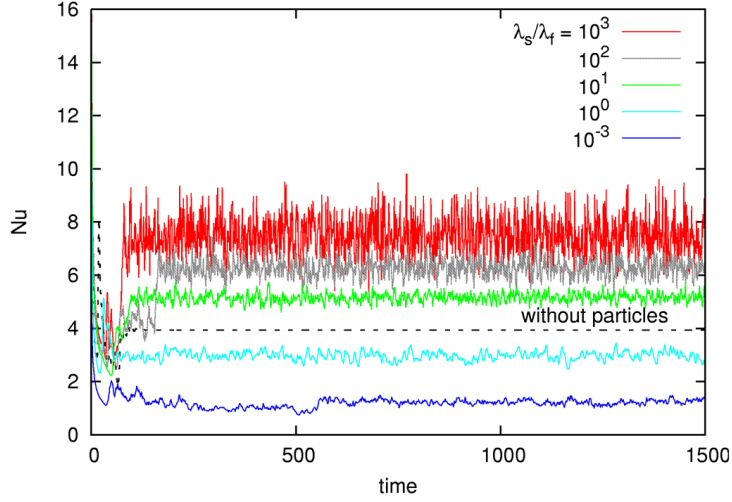


Figure 5: Comparison of time evolutions of Nusselt number for different ratios of heat conductivity. Solid volume fraction is 38.5%.

Dilute case with bulk solid volume fraction 6.54% (3-D)

Our method is extended to 3-D liquid-solid two-phase flow of Rayleigh number 10^5 . Figure 6 is an example of an instantaneous flow field including 5^3 spherical particles of $\lambda_g/\lambda_f = 10^2$ in a cubic domain. The other parameters are summarised in Table 2. The bulk solid volume fraction is 6.54%. The particles and fluid move randomly in the initial developing stage. After that, the particles and fluid are found to constantly circulate in one direction around the domain centre. Our preliminary study shows that, for different λ_g/λ_f and Rayleigh numbers, characteristic flow behaviours (such as circulating mode and weak oscillating mode) are observed.

Table2: Simulation parameters.

Number of grids	$N_x \times N_y \times N_z$	$100 \times 100 \times 100$
Spatial resolution	D_p/Δ	10
Number of particles	N_p	5^3
Rayleigh number	Ra	1.0×10^5
Diameter of particles	D_p	$0.1L$

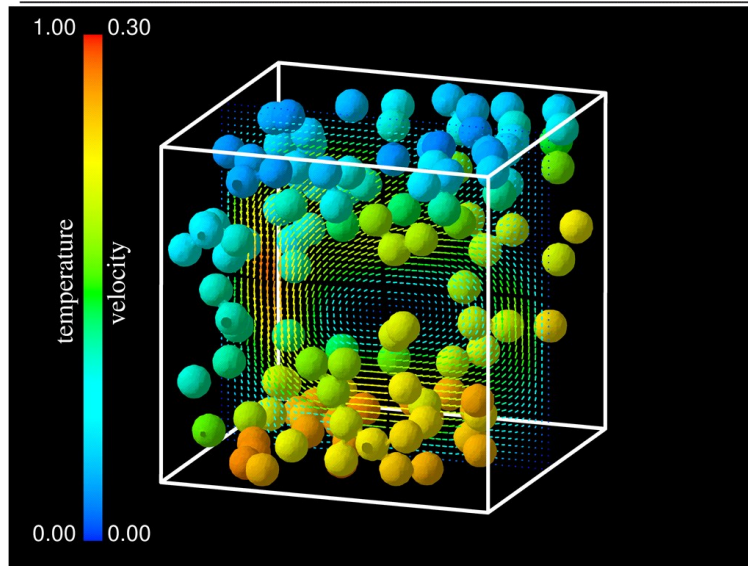


Figure 6: Instantaneous flow field and contours of temperature for different heat conductivities. Rayleigh number is 10^5 and bulk solid volume fraction is 6.54%. Temperature distribution on the surface of each particle and velocity vectors in a vertical cross section.

Conclusions

To simulate solid-dispersed two-phase flow with heat transfer, a method considering the effects of temperature distribution within a particle was developed based on our original immersed solid and a discrete-element methods.

The method is applied to 2-D and 3-D liquid-solid two-phase flow under a relatively low Rayleigh number. In the dense condition (2-D), the particles of a high heat conductivity induce the heat convection of the fluid, and promote the heat transfer of the system. On the other hand, for the low heat conductivity case, the particles concentrate in the near-wall regions and intercept the heat transfer from the hot wall to the fluid, resulting in low Nusselt number.

These results highlight the effect of temperature distributions within the particles as well as liquid on the overall heat transfer performance in the multiphase flow.

References

- Kajishima, T., Takiguchi, S., Hamasaki, H. and Miyake, Y. (2001), Turbulence structure of particle-laden flow in a vertical plane channel due to vortex shedding. *JSME International Journal, Series B* 44-4, pp. 526-535.
- Kajishima, T. and Takiguchi, S. (2002), Interaction between particle clusters and fluid turbulence. *International Journal of Heat and Fluid Flow*, 23-5, pp. 639-646.
- Kajishima, T. (2004), Influence of particle rotation on the interaction between particle clusters and particle-induced turbulence. *International Journal of Heat and Fluid Flow*, 25-5, pp. 721-728.
- Kim, J., Kim, D. and Choi, H. (2001), An immersed-boundary finite-volume method for simulation of flow in complex geometries. *Journal of Computational Physics*, 171, pp. 132-150.
- Kim, J. and Choi, H. (2004), An immersed-boundary finite-volume method for simulation of heat transfer in complex geometries. *KSME International Journal*, 18, pp. 1026-1035.
- Nishiura, D., Shimosaka, A., Shirakawa, Y. and Hidaka, J. (2006), Hybrid Simulation of Hindered Settling Behaviour of Particles Using Discrete Element Method and Direct Numerical Simulation (in Japanese). *Kagaku Kogaku Ronbunshu*, 32-4, pp. 331-340.
- Pacheco, J.R., Pacheco-Vega, A., Rodić, T. and Peck, R.E. (2005), Numerical Simulations of Heat Transfer and Fluid Flow Problems Using an Immersed-Boundary Finite-Volume Method on Nonstaggered Grids. *Numerical Heat transfer, Part B* 48, pp. 1-24.
- Pacheco-Vega, A., Pacheco, J. R. and Rodić, T. (2007), A general scheme for the boundary conditions in convective and diffusive heat transfer with immersed boundary methods. *Journal of Heat Transfer*, 129, Issue 11, pp. 1506-1516.
- Ren, W.W., Shu, C., Wu, J. and Yang, W.M. (2012), Boundary condition-enforced immersed boundary method for thermal flow problems with Dirichlet temperature condition and its applications. *Computers & Fluids*, 57, pp. 40-51.
- Tsuji, Y., Kawaguchi, T. and Tanaka, T. (1993), Discrete particle simulation of two-dimensional fluidized bed. *Powder Technology*, 77, pp. 79-87.
- Ueyama, A., Moriya, S., Nakamura, M. and Kajishima, T. (2011), Immersed Boundary Method for Liquid-Solid Two-Phase Flow with Heat Transfer. *Transaction of JSME, Series B* 77-775, pp. 803-814.
- Yu, Z., Shao, X. and Wachs, A. (2006), A fictitious domain method for particulate flows with heat transfer. *Journal of Computational Physics*, 217, pp. 424-452.
- Yuki, Y., Takeuchi, S. and Kajishima, T. (2007), Efficient immersed boundary method for strong interaction problem of arbitrary shape object with the self-induced flow. *Journal of Fluid Science and Technology*, 2-1, pp. 1-11.